Computational 3D resolution enhancement for optical coherence tomography with a narrowband visible light source

de Wit, Jos; Glentis, George Othon; Kalkman, Jeroen

DOI
10.1117/12.2670226

Publication date
2023

Document Version
Final published version

Published in
Optical Coherence Imaging Techniques and Imaging in Scattering Media V

Computational 3D resolution enhancement for optical coherence tomography with a narrowband visible light source

Jos de Wit, George-Othon Glentis, Jeroen Kalkman

Jos de Wit, George-Othon Glentis, Jeroen Kalkman, "Computational 3D resolution enhancement for optical coherence tomography with a narrowband visible light source," Proc. SPIE 12632, Optical Coherence Imaging Techniques and Imaging in Scattering Media V, 126321E (11 August 2023); doi: 10.1117/12.2670226

SPIE.

Event: European Conferences on Biomedical Optics, 2023, Munich, Germany

Computational 3D resolution enhancement for optical coherence tomography with a narrowband visible light source

Jos de Wit[1], **George-Othon Glentis**[2], **and Jeroen Kalkman**[1,*]

[1] *Department of Imaging Physics, Technical University Delft, Lorentzweg 1, 2028 CJ, Delft, The Netherlands*
[2] *Department of Informatics and Telecommunications, University of Peloponnese, Tripolis, 22100 Greece*

[*] *j.kalkman@tudelft.nl*

Abstract: Phase-preserving spectral estimation optical coherence tomography (SE-OCT) enables combining axial resolution improvement with computational depth of focus (DOF) extension. We combine SE-OCT with interferometric synthetic aperture microscopy (ISAM) to obtain a high 3D resolution over a large depth range with a narrow bandwidth visible light super-luminescent diode (SLD). SE-OCT gives a five times axial resolution improvement to 1.5 micrometer. The combination with ISAM gives a sub-micron lateral resolution over a 300 micrometer axial range, 12 times the conventional DOF. The results show that phase-preserving SE-OCT is sufficiently accurate for coherent post-processing, enabling the use of cost-effective SLDs in the visible light range for high spatial resolution OCT.

1. Introduction

The lateral resolution in optical coherence tomography (OCT) can be improved by using shorter wavelengths or by increasing the numerical aperture (NA) of the focusing lens. Increasing the NA reduces the depth of focus (DOF) quadratically, while reducing the wavelength decreases the DOF linearly. Thus, for obtaining lateral resolutions around or below a single micrometer the use of a high NA and a short wavelength leads to a very small DOF. The DOF can be computationally expanded using, for example, interferometric synthetic aperture microscopy (ISAM) [1]. Moreover, as the DOF reduction is less severe with wavelength reduction (linearly) than with increasing the NA (quadratically), and increasing the NA causes other problems such as a reduced working distance and a more complex optical design, using light with short wavelength in the visible range is preferred over further increasing the NA.

Most reported VIS SD-OCT system use supercontinuum (SC) lasers as light source [2], which, with their large bandwidth provide a high axial resolution. However, SC sources are expensive, suffer from relative intensity noise and require strict laser safety measures. Super luminescent diodes (SLDs) have much lower noise and are cheaper. However, the few SLDs in the VIS range that are available, have a narrow bandwidth. Previous applications to OCT use two such SLDs combined with deep learning [3], or have a poor 12 μm axial resolution.

Spectral estimation OCT (SE-OCT) can improve the axial resolution beyond the conventional bandwidth limit [4]. Contrary to other methods, such as auto-regressive (AR) estimation, the iterative adaptive approach (IAA) preserves the phase information of the OCT reconstruction. This enables the use of coherent methods for DOF extension. Here, we demonstrate a high resolution in 3D over a large depth range by combining SE-OCT with ISAM. As ISAM is implemented as an interpolation in spatial frequency domain, SE-OCT is effectively an extrapolation of the data in wavenumber space. We use missing-data IAA (MIAA) [5] to do this extrapolation explicitly, and apply ISAM afterwards to obtain good quality results.

2. Theory and methods

Figure 1 gives a schematic overview of the combined IAA and ISAM processing pipeline. First, the axial resolution is improved with RFIAA, which is then used to extrapolate the spectral data (i.e. computational bandwidth extension) with MIAA. After a lateral Fourier transform, the data is in k-space, where ISAM is applied by interpolated along the curves with constant axial scattering wavenumber $k_z(k,k_x,k_y)$. The 3D IFFT yields an image with high resolution in 3D.

IAA uses a weighted least square method to obtain a high resolution estimate of reflectivity $a(z_l)$ at depth z_l:

$$a(z_l) = \mathrm{argmin}_{a(z_l)} \left|\mathbf{y}_g - a(z_l)\mathbf{f}_g(z_l)\right|^2_{\mathbf{Q}_g^{-1}(z_l)}, \quad l = 0,1,\ldots,L-1, \tag{1}$$

where $\mathbf{y}_g$ is the measured and uniformly reshaped interference spectrum, $\mathbf{f}_g(z_l) = \left[\mathrm{e}^{-2\pi i z_l k_0} \ \ldots \ \mathrm{e}^{-2\pi i z_l k_{N_g}}\right]^T$ is the vector with corresponding Fourier components, and $Q_g(z_l)$ is the covariance matrix of the data, excluding that for z_l. The inverse of the covariance matrix suppresses the contribution of high intensity reflectivity to depths other

Optical Coherence Imaging Techniques and Imaging in Scattering Media V, edited by Benjamin J. Vakoc, Maciej Wojtkowski, Yoshiaki Yasuno, Proc. of SPIE Vol. 12632, 126321E
© 2023 SPIE · 0277-786X · doi: 10.1117/12.2670226

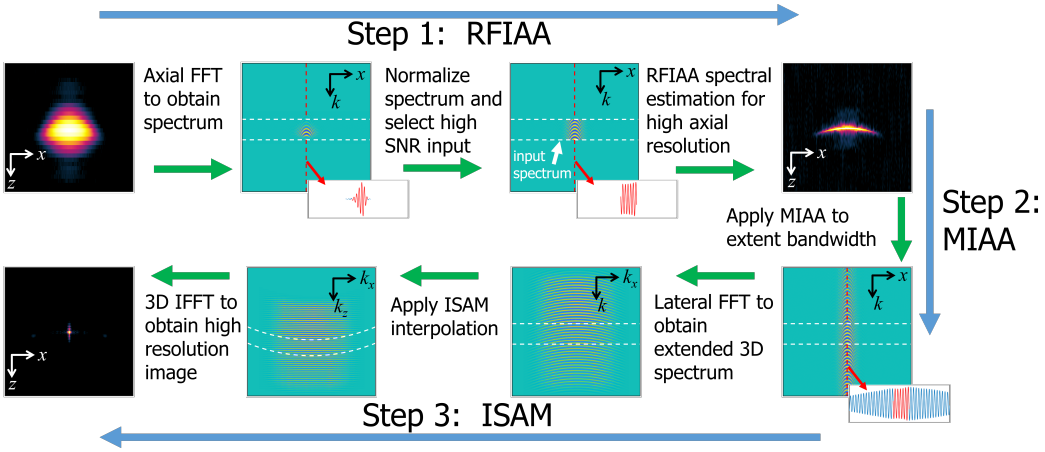

Fig. 1. Schematic figure of the proposed method. The white dashed lines indicate the edges of the input spectrum for RFIAA spectral estimation OCT. The line plots are the spectrum in at the center (red-dashed line), with the RFIAA input spectrum in red.

than the estimated one, thus reducing side-lobes and the main-lobe width. The solution for Eq. (1) is

$$a(z_l) = \frac{\mathbf{f}_g(z_l)^H \mathbf{R}_g^{-1} \mathbf{y}_g}{\mathbf{f}_g^H(z_l) \mathbf{R}_g^{-1} \mathbf{f}_g(z_l)}, \quad l = 0, 1, \ldots, L-1, \tag{2}$$

where

$$\mathbf{R}_g = \sum_{l=0}^{L-1} |a(z_l)|^2 \mathbf{f}_g(z_l) \mathbf{f}_g^H(z_l) + \Sigma \tag{3}$$

is the estimate of the data covariance matrix. Iterating 10 times between Eqs. (2) and (3) after initiating with $\mathbf{R}_g = \mathbf{I}$ (i.e. uniform weighting) refines the estimate resulting in a high resolution estimate of the reflectivity. The extrapolated spectrum $\mathbf{y}_m$ (i.e. the missing spectral data), is then obtained with

$$\mathbf{y}_m = \mathbf{T}\mathbf{y}_g = \left(\mathbf{R}_{mg}\mathbf{R}_g^{-1}\right)\mathbf{y}_g, \tag{4}$$

where $\mathbf{R}_{mg}$ is the cross-covariance matrix that is from $a(z_l)$ in a way similar to Eq. (3), but also including $\mathbf{f}_m(z_l)$, the Fourier vector with the missing data wavenumbers k_n.

ISAM is applied by interpolating the data to a linear grid in axial wavenumber

$$k_z(k, k_x, k_y) = \sqrt{2k^2 - k_x^2 - k_y^2}, \tag{5}$$

where k_x and k_y are the lateral wavenumbers. The data in k is obtained after MIAA, the data in k_x and k_y is obtained after performing a 2D Fourier in the lateral x and y direction.

The custom build OCT setup uses a fiber-coupled SLD light source with 510 nm center wavelength and 7 nm bandwidth (FWHM) (EXS210118-01, Exalos). The light is split into a reference and sample arm with a fiber coupler/splitter. In the sample arm, the light is collimated, scanned with galvo mirrors, and focused on the sample with a scan lens, tube lens and microscope objective (10x Plan Apochromat, Mitutoyo) with an NA of 0.28. The 11.2 mm diameter aperture of the objective is slightly underfilled with a 9.4 mm waist Gaussian beam. The light is detected using a custom spectrometer with a bandwidth of 24.1 nm distributed over 3072 pixels. A sample of point scatterers fixed in gelatin is used to characterize the 3D resolution. A lettuce leaf is used as biological test sample. For both samples a lateral area of 0.225×0.225 mm is imaged with 512×512 scanlines. After k-linearization and dispersion correction and axial IFFT, an axial region of interest of 200 pixels is selected. The axial FFT of this data serves as input for the recursive fast IAA (RFIAA) algorithm. The low SNR edges of the spectra were discarded, such that 128 pixels remained as input for RFIAA. The spectrum was extrapolated to 800 pixels, corresponding to a 96 nm wide spectrum.

3. Results and discussion

A 3D Gaussian fit on scatterers in simulations-based images and the image from the point scatterer sample was used to characterize the resolution. The lateral resolution after ISAM was with around 0.8 µm around the theoretical value in focus, but now over a depth range of 300 µm; this is a 12 times improvement of the DOF. The axial resolution was improved from 8 µm Fourier transform limited resolution to a 1.5 µin focus (a factor 5), up to 4.5 µm at 150 µm away from focus (a factor 1.8). The depth-dependency of the axial resolution is related to less efficient MIAA estimation away from focus where the SNR is reduced.

Figure 2 shows the imaging results of the lettuce leaf. The close to isotropic resolution with MIAA+ISAM gives a clear improvement in OCT image quality with respect to conventional DFT + ISAM reconstruction (a, b). The

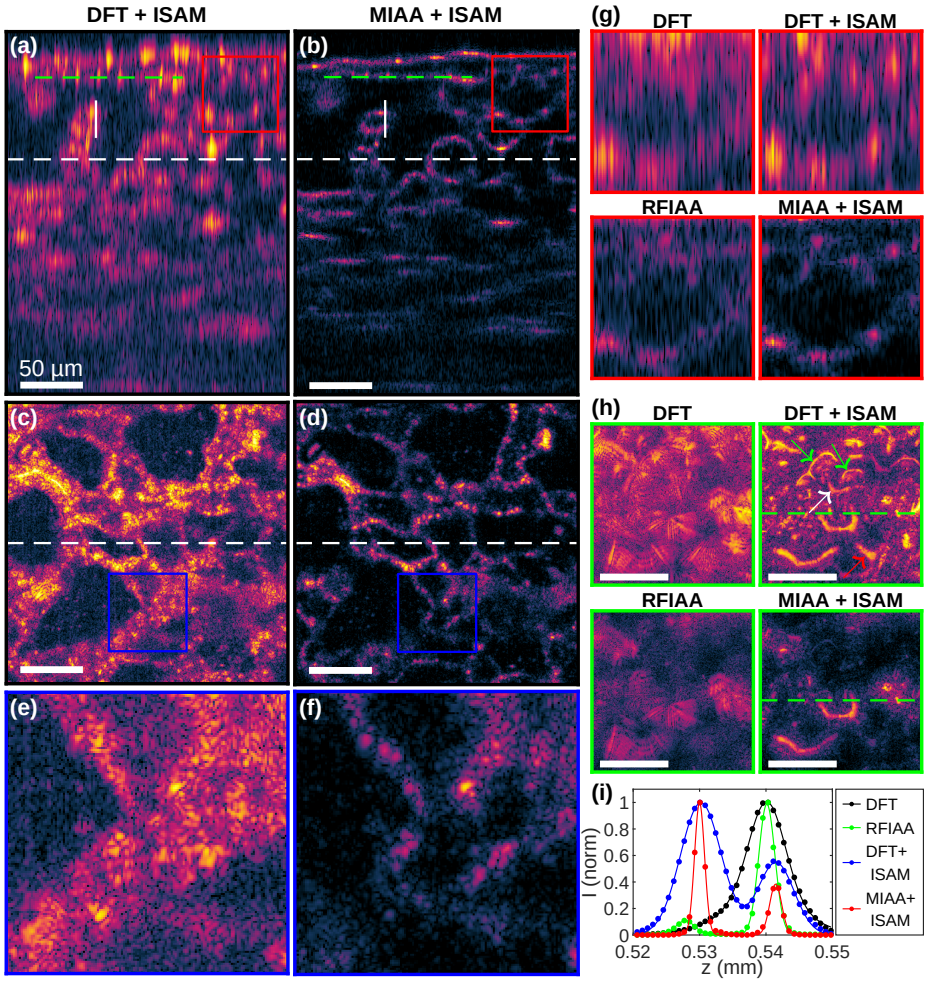

Fig. 2. Reconstruction results of the lettuce leaf. (a-f) compares DFT + ISAM with MIAA + ISAM. (a-b) An *xz*-cross section of the 3D leaf reconstruction. (c-d) The enface image at the white dashed line in (a-b), the white dashed line indicates intersection between (a-b) and (c-d). (e-f) A close-up of the blue square in (c-d). (g) The image at the red box in (a-b) for all four methods. (h) The enface image at the green dashed line in (a-b) for all four methods, the green dashed line indicates the intersection between the images of (a-b) and (h). (i) The A-scan at the vertical white line in (a-b) for all four methods, the line being a 2-peak Gaussian fit through the intensities.

improved optical sectioning ability is clear from the enface images (c-f), which have a much more open structure with MIAA + ISAM. Fig. 2(g) shows with a zoomed in section that small cellular structures are much better imaged with MIAA + ISAM than with the other methods, also at the top where RFIAA (without ISAM) gives a lateral blur. Fig. 2(h) shows the effect of ISAM away from the focal plane, where the images without ISAM (DFT and RFIAA) give a blurred signal. The A-scan in (i) shows that the axial resolution (FWHM) improves from 7.2 µm and 6.4 µm for DFT + ISAM to 1.8 µm and 2.1 µm for MIAA + ISAM, a factor 3 to 4 improvement.

The results show that the IAA-based SE-OCT can be used in combination with ISAM coherent processing to extent the depth of focus. We obtained a high micrometer resolution in 3D over a depth range of 300 micrometer.

References

1. Tyler S Ralston, Daniel L Marks, P Scott Carney, and Stephen A Boppart. Interferometric synthetic aperture microscopy. *Nature physics*, 3(2):129–134, 2007.
2. Xiao Shu, Lisa Jane Beckmann, and Hao F Zhang. Visible-light optical coherence tomography: a review. *Journal of biomedical optics*, 22(12):121707, 2017.
3. Antonia Lichtenegger et al. Reconstruction of visible light optical coherence tomography images retrieved from discontinuous spectral data using a conditional generative adversarial network. *Biomedical Optics Express*, 12(11):6780–6795, 2021.
4. Jos De Wit, Kostas Angelopoulos, Jeroen Kalkman, and George-Othon Glentis. Fast and accurate spectral-estimation axial super-resolution optical coherence tomography. *Optics Express*, 29(24):39946–39966, 2021.
5. Petre Stoica, Jian Li, Jun Ling, and Yubo Cheng. Missing data recovery via a nonparametric iterative adaptive approach. In *2009 IEEE International Conference on Acoustics, Speech and Signal Processing*, pages 3369–3372. IEEE, 2009.